15th International Congress on Artificial Materials for Novel Wave Phenomena - Metamaterials 2021
New York, USA, Aug. 2$^{\text{nd}}$ - 7$^{\text{th}}$ 2021

Deep sub-wavelength vortices by nonlinear mixing

N. Jiménez[1], J. Ealo[2], R. Muelas-Hurtado[2], A. Duclos[3] and V. Romero-García[3]

[1]Instituto de Instrumentación para Imagen Molecular (I3M), Universitat Politècnica de València - CSIC, València, Spain
[2]School of Mechanical Engineering, Universidad del Valle, Cali, Colombia
[3]Laboratoire d'Acoustique de l'Université du Mans (LAUM), UMR CNRS 6613, Institut d'Acoustique - Graduate School (IA-GS), CNRS, Le Mans Université, France
vicente.romero@univ-lemans.fr

***Abstract* – Using the nonlinear self-demodulation of two confocal vortices, we report the generation of acoustic vortices of deep sub-wavelength dimensions. A helicoidal acoustic source with two different slopes is used to generate two primary focused vortices beams with finite amplitude of different frequencies and topological charges. The self-demodulated vortex presents the spatial distribution of the main vortices with a sub-wavelength size when compared to its wavelength. Nonlinearity enables the generation of focused vortex beams of tunable topological charge in the far-field whose characteristic size is 22 times smaller than its wavelength.**

I. Introduction

Vortex beams are characterized by a collimated wavefront with a phase dependence of the type $e^{\imath l\phi}$, with ϕ the azimuthal angle and l the topological charge, respectively. At the principal axis of the vortex beam the field exhibits a phase singularity and the field is null. Methods to synthesize these beams include active devices such as phased arrays [2], helical radiating surfaces [1] or Archimedean [3] or Fresnel spiral diffraction gratings [4] among others. Metamaterials have also been used to generate vortex beams by using flat and sub-wavelength structures [6]. However, in all these configurations the natural diffraction of the wavefront limits the size of the vortex. ~~The minimum value is only reached for distances smaller than the Rayleigh diffraction length of the source due to the divergence of the beam, given by the relation between the geometry of the source and the wavelength.~~ Recently, increasing attention has been paid to restoring the evanescent components of a field to overcome the diffraction limit either using metamaterials [7] or time-reversal techniques [5]. However, as these approaches rely on evanescent waves, their use is restricted to near-field distances.

In this work, we synthesize a vortex beam of sub-wavelength size at a distance beyond Rayleigh diffraction length using the nonlinear mixing of two confocal, high-frequency and detuned vortex beams of different topological charges. We demonstrate the concept using the natural self-demodulation phenomenon in air. We generate a focused vortex beam of integer topological charge whose distance between magnitude maxima is ~ 18 times smaller than its wavelength at a distance ~ 2.8 times the Rayleigh diffraction length.

II. Results

A device was manufactured by disposing 10-mm diameter ultrasound emitters operating in air over two different helical surfaces as shown in Figs. 1(a-b). The helical profile of the n-th surface (with $n = 1, 2$) was designed to generate a focused beam at a focal point, $\mathbf{r}(\phi, r, z) = (0, 0, F)$, and, simultaneously, produce at this location a difference of time of flight equal to $\Delta t_n = l_n\phi/\omega_n$, where l_n is the topological charge of the n-the primary vortex beam, ω_n the angular frequency and ϕ the azimuthal coordinate. In particular, the first source, composed of the two internal concentric rings of transducers, see Fig. 1(b), was excited with a sinusoidal pulse burst of $\omega_1/2\pi = 40$ kHz while the second one, composed of the two external concentric rings of transducers, was excited at $\omega_2/2\pi = 41$ kHz. Figure 1(c) and (d) show the sagittal field cross-sections at $y = 0$ experimentally measured for the two primary beams respectively. The topological charges of the primary vortex beams, defined by the curvature of the

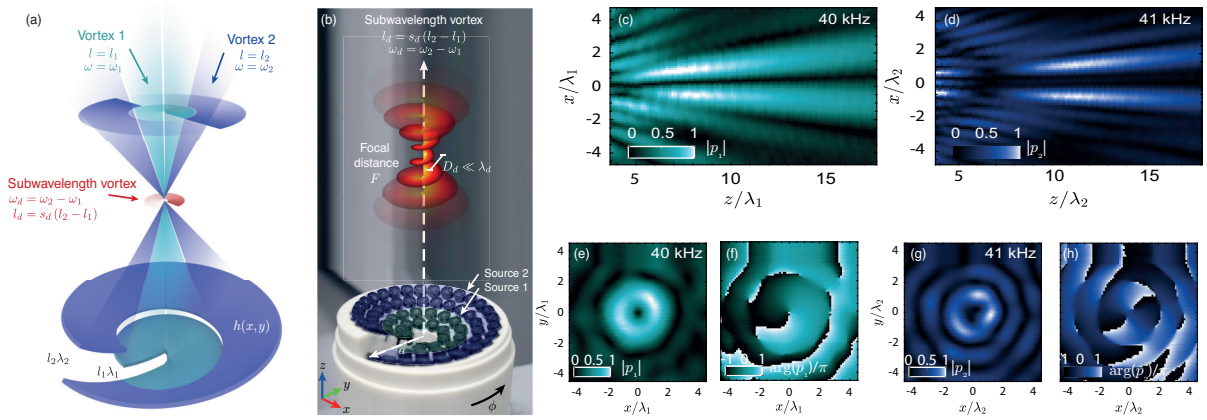


Fig. 1: (a) Scheme of the system composed of two confocal focused vortex beams at frequencies ω_1 and ω_2, with topological charges l_1 and l_2, respectively. Self-demodulation is generated by nonlinearity, producing a vortex at the difference frequency $\omega_d = \omega_2 - \omega_1$, with a topological charge of $l_d = l_2 - l_1$ and a beam-width given by D_d in the sub-wavelength regime. (b) Photograph of the helical source used in the experiments. (c) and (d) show the sagittal field cross-sections at $y = 0$, experimentally measured, showing the magnitude of the acoustic field ($|p_i|$) at frequencies 40 kHz and 41 kHz respectively. (e-h) Transverse field cross-section at $z = 80$ mm, experimentally measured, showing the normalized magnitude ($|p_i|$) and the normalized phase ($\arg(p_i)/\pi$) of the acoustic field at frequencies 40 kHz and 41 kHz respectively.

helical surfaces, were set to $l_1 = 1$ and $l_2 = 2$ (as shown by Fig. 1(f) and (h)). Source aperture was set to $2a = 110$ mm, with a the radius of the source, and the focal point was $F = 100$ mm. Thus, the Rayleigh distances for the primary vortex beams are around $\pi a^2/\lambda_1 \approx \pi a^2/\lambda_2 \approx 1.1$ m.

For finite-amplitude waves, and when all emitters are active, both beams interact and due to material and advective nonlinearity wave mixing occurs during propagation. Higher harmonics arise as arithmetical combinations of the fundamental waves of both beams. In addition to higher harmonics, a difference-frequency mode of frequency $\omega_d = \omega_2 - \omega_1$ is generated due to the nonlinear self-demodulation of the beating wavefront.

As homogeneous acoustic media lack of strong dispersion, phase-matching holds during nonlinear propagation and harmonic generation processes are cumulative with distance. On the one hand, it is expected that the locally-generated self-demodulated mode presents a field spatial distribution similar to those of the primary beams, as occurs in parametric acoustic antennas [9]. On the other hand, the phase of the self-demodulated beam depends on the spatio-temporal interference of the two vortex beams, which is linked to their topological charges. This results in a self-demodulated beam with a phase factor $\exp(il_d\phi)$ where the topological charge of the self-demodulated beam is $l_d = s_d(l_2 - l_1)$, where $s_d = \text{sign}(\omega_2 - \omega_1)$, due to the conservation of topological charge of nonlinear vortices, which is indeed a consequence of the conservation of angular momentum [8].

Simulated and experimental results for the self-demodulated component are shown in Fig. 2. A low-frequency beam at $\omega_d = 1$ kHz is generated locally, and its spatial distribution matches the overlapping volume of the two primary beams. Its corresponding wavelength is $\lambda_d = 2\pi c_0/\omega_d \gg \lambda_n$, therefore, the width of the beam, dominated by the width of the primary beams, is sub-wavelength. The magnitude and the phase distributions of the self-demodulated component is shown in Figs. 2 (c-f). Its topological charge is given by $l_d = l_2 - l_1 = 1$, showing the conservation of topological charge and, therefore, the conservation of orbital angular momentum during the nonlinear mixing of the primary beams.

Figure 2(g) shows the transversal pressure-field distribution of the self-demodulated vortex beam at $z = 80$ mm and $y = 0$ mm. The width of the vortex, D_d, is 17.9 times smaller than the wavelength in the experimental observations ($D_d = \lambda_d/22.2$ in simulations). Note that the measurement distance is 2.8 times the Rayleigh diffraction length for the self-demodulated mode. The field at the axis ($x = 0$) becomes null due to the phase singularity. The phase of the beam along the azimuthal coordinate ϕ, depicted in the input of Fig. 2(g), agrees with a linear profile of $(l_2 - l_1)\phi = l_d\phi$, demonstrating the topological charge conservation during nonlinear mixing.

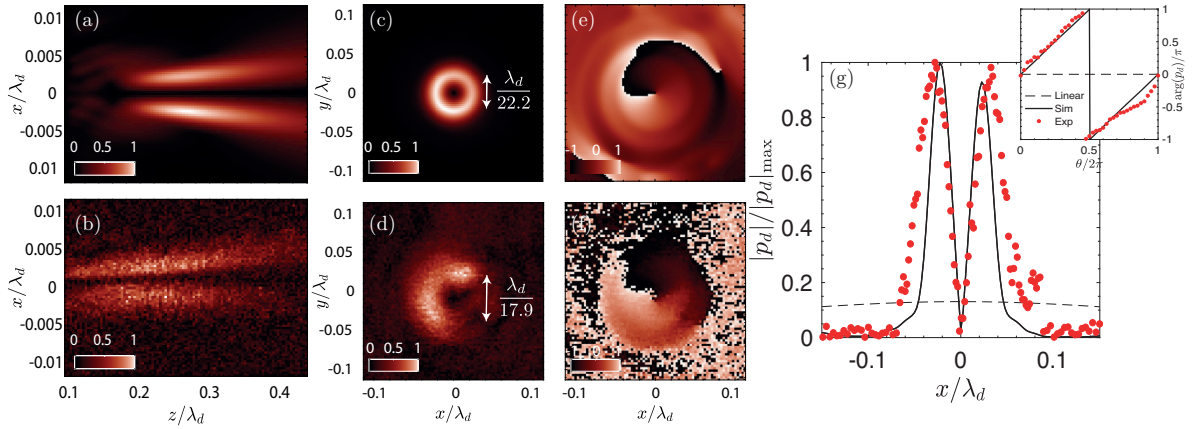


Fig. 2: (a) and (b) show the sagittal field cross-sections at $y = 0$ showing $|p_d|$ of the theoretical and measured demodulated component respectively. (c-f) Transverse field cross-section at $z = 80$ mm showing the normalized magnitude ($|p_d|$) and the normalized phase ($\arg(p_d)/\pi$) of the theoretical and measured demodulated component respectively. (g) Normalized field magnitude cross-section $p(x, y = 0, z = 80$ mm$)$ at 1 kHz obtained experimentally, numerically and by linear theory. Input: Phase of the self-demodulated field along the azimuthal coordinate.

III. Conclusion

In this work we have shown the sub-wavelength and sub-diffractive generation of acoustic vortices at distances beyond Rayleigh diffraction length by using the nonlinear self-demodulation. Sub-wavelength vortices emerge as a result of the spatio-temporal interference of two primary vortex beams due to the conservation of angular momentum during nonlinear wave-mixing.

Acknowledgement

This research has been supported by the Spanish Ministry of Science, Innovation and Universities through grants "Juan de la Cierva - Incorporación" IJC2018-037897-I and PID2019-111436RB-C22, by the Agència Valenciana de la Innovació through grants INNVA1/2020/92 and INNCON/2021/8, and by HYPERMETA funded by Région Pays de la Loire. R.D.M.-H acknowledges support from Colciencias Scholarship program No. 727-2015.

References

[1] Joao L Ealo, Jose Carlos Prieto, and Fernando Seco. Airborne ultrasonic vortex generation using flexible ferroelectrets. *IEEE Trans. Ultrason. Ferroelectr. Freq. Control*, 58(8):1651–1657, 2011.

[2] Brian T Hefner and Philip L Marston. An acoustical helicoidal wave transducer with applications for the alignment of ultrasonic and underwater systems. *Jour. Acous. Soc. Am.*, 106(6):3313–3316, 1999.

[3] Noé Jiménez, Rubén Picó, Víctor Sánchez-Morcillo, Vicent Romero-García, Lluís M García-Raffi, and Kestutis Staliunas. Formation of high-order acoustic Bessel beams by spiral diffraction gratings. *Phys. Rev. E*, 94(5):053004, 2016.

[4] Noé Jiménez, Vicent Romero-García, Luis M García-Raffi, Francisco Camarena, and Kestutis Staliunas. Sharp acoustic vortex focusing by Fresnel-spiral zone plates. *Appl. Phys. Lett.*, 112(20):204101, 2018.

[5] Geoffroy Lerosey, Julien De Rosny, Arnaud Tourin, and Mathias Fink. Focusing beyond the diffraction limit with far-field time reversal. *Science*, 315(5815):1120–1122, 2007.

[6] A Marzo, A Ghobrial, L Cox, M Caleap, A Croxford, and BW Drinkwater. Realization of compact tractor beams using acoustic delay-lines. *Appl. Phys. Lett.*, 110(1):014102, 2017.

[7] John Brian Pendry. Negative refraction makes a perfect lens. *Phys. Rev. Lett.*, 85(18):3966, 2000.

[8] Jean-Louis Thomas and Régis Marchiano. Pseudo angular momentum and topological charge conservation for nonlinear acoustical vortices. *Phys. Rev. Lett.*, 91(24):244302, 2003.

[9] Peter J Westervelt. Parametric acoustic array. *Jour. Acous. Soc. Am.*, 35(4):535–537, 1963.